Impact of G2 checkpoint defect on centromeric instability

Wen Deng[1], Ph.D.; Sai Wah Tsao[1], Ph.D.; Grace W.Y. Mak[1], M.Phil; Chi M. Tsang[1], Ph.D.; Wilson Y. P. Ching[1], Ph.D.; Xin-Yuan Guan[2], Ph.D.; Michael S.Y. Huen[1], Ph.D.; and Annie L.M. Cheung[1,3], Ph.D.

[1]Department of Anatomy and [2]Department of Clinical Oncology, Li Ka Shing Faculty of Medicine, The University of Hong Kong, Hong Kong, SAR, China

[3]Correspondence
Dr. Annie L. M. Cheung
Department of Anatomy, The University of Hong Kong,
Faculty of Medicine Building, 21 Sassoon Road, Pokfulam, Hong Kong, China
Tel. No. (852) 28199293 Fax No. (852) 28170857
Email: lmcheung@hkucc.hku.hk

Running title: G2 phase defect promotes centromeric instability

Abstract

Centromeric instability is characterized by dynamic formation of centromeric breaks, deletions, iso-chromosomes and translocations, which are commonly observed in cancer. So far, however, the mechanisms of centromeric instability in cancer cells are still poorly understood. In this study, we tested the hypothesis that G2 checkpoint defect promotes centromeric instability. Our observations from multiple approaches consistently support this hypothesis. We found that overexpression of cyclin B1, one of the pivotal genes driving G2 to M phase transition, impaired G2 checkpoint and promoted the formation of centromeric aberrations in telomerase-immortalized cell lines. Conversely, centromeric instability in cancer cells was ameliorated through reinforcement of G2 checkpoint by cyclin B1 knockdown. Remarkably, treatment with KU55933 for only 2.5 h, which abrogated G2 checkpoint, was sufficient to produce centromeric aberrations. Moreover, centromeric aberrations constituted the major form of structural abnormalities in G2 checkpoint-defective ataxia-telangiectasia (A-T) cells. Statistical analysis showed that the frequencies of centromeric aberrations in G2 checkpoint-defective cells were always significantly overrepresented compared with random assumption. Since there are multiple pathways leading to G2 checkpoint defect, our finding offers a broad explanation for the common occurrence of centromeric aberrations in cancer cells.

Key words: G2 checkpoint, defect, centromere, instability

Introduction

Centromeres are integral chromosomal elements where sister chromatids are constricted and the microtubules are attached for chromosome segregation during cell division. Investigations on chromosomal structural dynamics indicate that centromeres, being hotspots for rearrangements during species evolution, are intrinsically predisposed to instability (Eichler and Sankoff, 2003). Cytogenetic studies have shown that centromeric or pericentromeric aberrations such as whole-arm translocations, deletions and iso-chromosomes are common in human cancer cell lines and primary solid tumors of various origins (Jin et al., 1995; Zhu et al., 1995; Johansson et al., 1995; Beheshti et al., 2000; Wong et al., 2000; Padilla-Nash et al., 2001). The frequent occurrence of centromeric aberrations in tumor cells suggests that centromeric instability may contribute to tumor development. However, the mechanisms of centromeric instability in carcinogenesis remain poorly understood. Elevated levels of centromeric instability are well characterized in ICF (immunodeficiency, centromeric region instability, facial anomaly) patients, and are ascribed to hypomethylation of centromeric DNA, leading to centromeric aberrations specifically on chromosomes 1, 16, and sometimes 9 (Ehrlich, 2002). Yet, centromeric aberrations in most human tumors are not limited to the three chromosomes. Therefore, other mechanisms are probably involved in the genome-wide centromeric instability in tumor cells.

Human centromeres consist largely of repeated short sequences known as α-satellite DNA sequences, which are tightly packed into centromeric heterochromatin. It has been proposed that the condensed structure of heterochromatin presents barriers to DNA replication such that replication fork stalling occurs; and unresolved stalled replication

forks may generate DNA double-strand breaks (Leach et al., 2000). In normal cells, the G2 checkpoint exerts its protective function by delaying cell cycle progression from G2 to M phase to provide time for correction of post-replication errors and DNA damage repair. We therefore hypothesize that centromeric DNA may be preferentially subject to erroneous replication that fails to be corrected in cells with defective G2 checkpoint, leading to centromeric instability. Cyclin B1 is one of the specific and pivotal genes driving G2 to M phase transition. The overexpression of cyclin B1 is expected to induce G2 checkpoint defect. In this study, for the first time, we obtained the evidence that defective G2 checkpoint, induced by manipulation of cyclin B1 overexpression and inhibition of its upstream regulator ATM (ataxia telangiectasia-mutated), indeed promotes centromeric instability in the context of spontaneous DNA damage preferentially occurring at or near centromeres.

Results

Cyclin B1 overexpression promotes G2 checkpoint defect and centromeric instability

To study the causative role of G2 checkpoint defect in centromeric instability, we stably overexpressed cyclin B1 in two human telomerase-immortalized cell lines derived from normal esophageal epithelial cells (NE2-hTERT) (Cheung et al., 2010) and nasopharyngeal epithelial cells (NP460-hTERT) (Li et al., 2006), which were chosen because they had low background levels of centromeric instability. The cells were infected with retroviral plasmids expressing cyclin B1 or empty vector and selected with puromycin for 6 days. Western blotting analysis demonstrated the successful

overexpression of cyclin B1 (Figure 1a, lanes 1-4). This was also accompanied by the increased expression of active form of phospho-cdc2, p-cdc2(Thr161), which is known to form complex with cyclin B1 to promote G2 to M phase transition, while there was no remarkable change in the total levels of cdc2. Because intact G2 checkpoint enforces G2 arrest after DNA damage, the function of G2 checkpoint was readily monitored by the percentage of mitotic cells 2 h after 1 Gy γ-ray irradiation relative to that of un-irradiated control cells (i.e. relative mitotic index) (Xu et al., 2002; Terzoudi et al., 2005; Deckbar et al., 2007). We confirmed that the cyclin B-overexpressing cells had impaired G2 checkpoint function as evidenced by the higher relative mitotic indices (Figure 1a, lanes 1-4, and Table S1) compared with empty-vector infected cells after γ-ray irradiation, indicating inefficient G2 arrest after cyclin B1 overexpression.

Un-irradiated cells were analyzed for spontaneous chromosome aberrations using 24-color spectral karyotyping (SKY) and pan-centromere fluorescence *in situ* hybridization (FISH) at the 6th population doubling (PD) after puromycin selection. The most remarkable finding was a ~20-fold increase in the frequencies of non-clonal centromeric aberrations in cyclin B1 overexpressing cells compared with empty-vector infected cells (Figure 2, lanes 1-4). The new aberrations (Table S2) included centromeric chromatid breaks, centromeric chromosomal deletions, centromeric translocations and iso-chromosomes, as exemplified in Figure 3a. The centromeric aberrations were confirmed by the presence of centromere FISH signals at the broken ends or chromosome rejoining points (Figure 3a, right). These results represent the first direct evidence that G2 checkpoint defect promotes centromeric instability.

Cyclin B1 knockdown reinforces G2 checkpoint function and reduces centromeric instability in cancer cells

We next tested the impact of G2 checkpoint defect on centromeric instability in cancer cells. Three cancer cell lines of different cell types: HeLa (cervical cancer), SLMT-1 (esophageal cancer) (Tang et al., 2001) and HNE-1 (nasopharyngeal cancer) (Glaser et al., 1989) were examined. Although cancer cells are known to retain some degree of G2 checkpoint function, we anticipated that the G2 checkpoint in cancer cells may not be as stringent as in normal cells. To obtain normal control cells, we cultured primary epithelial cells from normal tissues donated by 6 independent individuals (NC104 and NC105 for cervical epithelial cells, NP601 and NP602 for nasopharyngeal epithelial cells, NE1 and NE6 for esophageal epithelial cells). SKY analysis confirmed that an average of 98% of these primary epithelial cells had a normal karyotype. Western blotting analysis showed that the control cells had significantly lower protein expression of cyclin B1, active form of phospho-cdc2 and total cdc2 than the cancer cells (Figure 1a, lanes 5-7, 12-14, and 19-21). The relative mitotic indices of normal and cancer cells after γ-ray irradiation decreased to an average of 2 and 34%, respectively (Figure 1b, lanes 6-8, 12-14 and 18-20), demonstrating that the cancer cells had defective G2 checkpoint. Detailed mitotic indices are given in Table S3). Karyotype analysis revealed that each cancer cell line (un-irradiated and pooled culture) had specific clonal structural aberrations that were present in all analyzed metaphases. However, the cells from each cancer cell line also had high frequencies of non-clonal structural aberrations, which predominantly involved centromeric regions (Figure 2, lanes 8, 14, and 20, and Table S4), indicating severe centromeric instability. Strikingly, the majority of clonal structural aberrations in the

cancer cell lines were also centromeric aberrations. Examples of karyotypes of the three cell lines are shown in Figure S1.

To examine whether defective G2 checkpoint truly contributes to centromeric instability in the cancer cell lines, we reinforced G2 checkpoint function by cyclin B1 knockdown to see if centromeric instability could be reduced. RNA interference directed against cyclin B1 was performed using plasmids containing a human cyclin B1 sequence that, when expressed, forms a short-hairpin RNA (shRNA) which gets processed into a cyclin B1-specific short interfering RNA. Figure 1a (lanes 8, 9, 15, 16, 22 and 23) shows the effective knockdown of cyclin B1 protein expression in the three cancer cell lines measured at 24 and 72 h after the plasmid transfection. Interestingly, the active form of phospho-cdc2 protein expression also showed some degree of decrease, but not the total levels of cdc2. The cyclin B1 shRNA-transfected cells had significantly lower mitotic indices ($P < 0.05$, Table S3) and were more sensitive to γ-ray irradiation compared with parental and control plasmid-transfected cells (Figure 1b and Table S3), suggesting the improvement of G2 checkpoint function after cyclin B1 knockdown. To achieve sustained cyclin B1 knockdown, we repeated cyclin B1 shRNA plasmid transfections twice with an interval of 48 h, and the cells were harvested 72 h after the third transfection. By the time of harvest, the cells had been transfected with cyclin B1 shRNA or control plasmids for 7 d. We then analyzed metaphases for spontaneous chromosome abnormalities and found that total non-clonal centromeric aberrations in the cells with cyclin B1 knockdown decreased significantly ($P < 0.05$) to about 40% of that in the parental and control plasmid-transfected cell lines (Figure 2, lanes 9, 10, 15, 16, 21, 22 and Table S4), indicating the amelioration of centromeric instability. The decreased

centromeric aberrations included chromatid-type (chromatid breaks) and chromosome-type (chromosome deletions, iso-chromosomes, centromeric translocations, centromeric-to-telomeric fusions). Although the frequencies of chromatid-type aberrations were expected to decrease with the checkpoint improvement within a single G2 phase, new chromosome-type aberrations could be generated by rearrangements of chromatid-type aberrations after DNA replication in the next cell cycle. Therefore the decrease in frequencies of both centromeric chromatid-type and chromosome-type aberrations was observed in cells harvested on Day 7 (which allowed cell proliferation for multiple cell cycles) of cyclin B1 knockdown. The frequencies of other non-clonal, non-centromeric aberrations also showed a trend of decrease but to a lesser extent than centromeric aberrations (Figure 2, lanes 9, 15 and 21). Taken together, the above data enabled us to conclude that G2 checkpoint defect induced by cyclin B1 overexpression plays an important role in the manifestation of centromeric instability in cancer cells.

We also studied the growth kinetics of cancer cells under cyclin B1 knockdown. By day 7, the numbers of cells transfected with cyclin B1 shRNA were about 50% that of cells transfected with control plasmids (Figure S2), indicating that cyclin B1 knockdown decreased cell proliferation rate by about one cell population doubling within 7 days of experiments. The slower population doubling of cancer cells after G2 checkpoint improvement with cyclin B1 knockdown might offer a trivial explanation for the reduction of centromeric and non-centromeric non-clonal aberrations.

G2 checkpoint defect induced by ATM inhibitor promotes centromeric instability

We then examined whether the upstream regulator of cyclin B1 also affects centromere instability. It is well-established that ATM is essential in maintaining G2 checkpoint

function (Terzoudi et al., 2005; Deckbar et al., 2007) through inhibition of cyclin B1/cdc2 (Abraham, 2001). We therefore examined the effect of a specific and potent ATM inhibitor, KU55933 (Rainey et al., 2008), which is known as a "molecular switch" because of its rapid and reversible inactivation of ATM (White et al., 2008), on centromeric instability. Being aware that ATM also has G1/S checkpoint functions (Abraham, 2001), we particularly designed experiments to examine the effect of KU55933 treatment without the confounding factor of G1/S checkpoint inactivation. The NE2-hTERT and NP460-hTERT cells were treated with 10 μM KU55933 or DMSO for 2.5 h, with the addition of colcemid 0.5 h after KU55933 or DMSO treatment to enable the collection of metaphases accumulated from G2 cells. The data in Figure 4a confirmed the G2 checkpoint inactivation by KU55933. An average of 11 non-clonal centromeric aberrations (mainly centromeric chromatid breaks) per 100 metaphases was detected after KU55933 treatment (Figure 4b and detailed data in Table S5). This frequency was 21-fold higher than that in control (DMSO-treated) cells (0.5 non-clonal centromeric aberrations per 100 metaphases). Other intra-arm aberrations were also induced by the inhibitor treatment but the frequencies were lower than centromeric aberrations (Figure 4b and Table S5). Because the total duration of the inhibitor treatment was only 2.5 h, and the duration of G2 phase of a typical human cell cycle lasts about 4 h even under the condition of ATM inhibition (Pincheira and Lopez-Saez, 1991), it is unlikely that the new aberrations in the metaphases after the transient inhibitor treatment stemmed from G1 or S phase. We therefore conclude that the centromeric aberrations can be induced by the ATM inhibition through the inactivation of G2 checkpoint function.

It is of interest to examine if the functions of ATM in G1 and S phases also play a role in regulating centromeric instability. We cultured NE2-hTERT and NP460-hTERT cells in KU55933- or DMSO-containing medium for 48 h (with medium change every 12 h). Colcemid was added into the culture medium 18 h before cell harvest to allow metaphase accumulation from G2, S and G1 phases. Chromosome aberration analysis showed ~ 30% increases in the frequency of non-clonal centromeric aberrations in both cell lines compared with 2.5 h treatment with KU55933 (Figure 4b and Table S5), indicating that G1/S checkpoint inactivation by ATM inhibition also induced centromeric instability but to a lesser extent than G2 checkpoint inactivation in the cell lines.

Human primary fibroblasts from A-T patients exhibit elevated centromeric instability

To further confirm the role of G2 checkpoint defect in centromeric instability, we used primary fibroblasts (without any ectopic gene expression) from patients with ataxia telangiectasia (A-T) syndrome, a cancer-prone disorder, to investigate whether these cells also show centromeric instability. The A-T cells were used as additional cell models because they are well-known to have defective G2 checkpoint due to the mutations in ATM and are frequently used in G2 checkpoint functional studies (Xu et al., 2002; Terzoudi et al., 2005; Deckbar et al., 2007). Analyses of relative mitotic indices after γ-radiation showed that the primary A-T cells from two patients (AG02496 and AG04405) had severe G2 checkpoint defect (Figures 4c). We found 55 and 72 spontaneous structural chromosome aberrations in 100 AG02496 and AG04405 metaphases, respectively, whereas ≤ 2 aberrations were detected in 100 primary fibroblasts derived from normal individuals. Strikingly, chromosome breakpoint analysis using SKY and centromere FISH showed that the majority of the aberrations in the un-irradiated A-T

cells occurred in centromeric regions (Figure 4d), producing centromeric chromatid breaks, whole-arm translocations, centromeric chromosomal deletions, iso-chromosomes, and another unexpected form described below.

Primary A-T cells are known to have telomeric instability (Pandita, 2002). Our analysis showed that these A-T cells not only had telomeric end-to-end fusions but also dicentrics formed by fusion between centromeric ends and telomeric ends (Figure 3b). The centromeric aberrations that were involved in fusions with telomeric ends accounted for about one fifth of the total centromeric aberrations in the A-T cells (Table S6). These results demonstrate that centromeric instability not only occurs independently but also cooperates with telomeric instability to generate complex genetic changes in G2 checkpoint-defective A-T cells. Although centromeric instability was not previously identified as a particular form of instability in A-T lymphocytes probably due to the high background of random genomic instability, previous cytogenetic analysis of A-T fibroblasts did show that centromeric or pericentromeric regions are hot-spots of breakage (Kojis et al., 1989), consistent with our results.

Statistical validation of significant overrepresentation of centromeric aberrations in G2 checkpoint-defective cells

Statistical analysis of the chromosome aberration data in Figure 2 showed that the frequencies of non-clonal centromeric aberrations were always significantly higher ($P < 0.05$) than those of non-centromeric aberrations in cyclin B1-overexpressing immortalized cells and G2 checkpoint-defective cancer cells (Figure 2, lanes 2, 4, 8, 10, 14, 16, 20, and 22). The frequencies of non-clonal centromeric aberrations in other G2 checkpoint-defective cells (KU55933-treated and A-T cells) were also higher than non-

centromeric aberrations (Figures 4b and 4d), although the differences were not statistically significant ($P > 0.05$). However, it is important to emphasize that the band ratio of centromeric (p11-q11) to non-centromeric bands is only about 0.27 in the male haploid genome (Stewenius et al., 2005). If the chromosome aberrations were randomly distributed along chromosomes, the expected ratio of centromeric aberrations to non-centromeric aberrations would be 0.27. Yet our experimental ratios of centromeric aberrations to non-centromeric aberrations in KU55933-treated and A-T cells (from male donors) ranged from 1.39 ± 0.38 to 2.00 ± 0.64 (Table 1), which were significantly ($P < 0.05$) higher than the expected value based on random assumption. These results together suggested that centromeric aberrations were significantly overrepresented in G2 checkpoint-defective cells.

Discussion

In this study, we uncovered a previously uncharacterized role of G2 checkpoint defect in chromosome instability. We have shown, for the first time, that defective G2 checkpoint preferentially promotes the manifestation of centromeric instability. Cyclin B1 is one of central and specific effector proteins driving G2 to M phase transition. We found that cyclin B1 overexpression in telomerase-immortalized cell lines compromised G2 checkpoint and increased the frequencies of non-clonal centromeric aberrations. We also showed that centromeric instability in cancer cells was associated with G2 checkpoint defect. Conversely, centromeric instability in cancer cells was reduced by G2 checkpoint improvement using cyclin B1 knockdown by RNA interference. We further demonstrated

that inhibition of ATM, the upstream regulator of cyclin B1/cdc2 and the well-recognized potent regulator of G2 checkpoint, induced *de novo* centromeric aberrations. It is important to note that although ATM also has G1 and S phase checkpoint functions, our experiments showed that transient (2.5 h) treatment with the specific ATM inhibitor, KU55933, was sufficient to induce centromeric aberrations. Because the treatment duration was shorter than G2 phase duration (usually lasts about 4 h), the confounding factor of G1/S phase checkpoint inhibition was avoided. Moreover, we analyzed detailed chromosome aberrations in primary fibroblasts derived from A-T patients. We particularly chose to test primary A-T cells because they are close to the *in vivo* situation and are frequently used in G2 checkpoint functional studies. We found that centromeric or pericentromeric aberrations were the most prominent form of spontaneous chromosome structural abnormalities in primary A-T fibroblasts. KU55933 treatments and ATM mutations also promoted non-centromeric chromosome instability, but to lesser extents than centromeric instability. Collectively, the above data lead us to conclude that G2 checkpoint defect plays a critical role in promoting centromeric instability.

It is envisaged that centromeric regions intrinsically present replication barriers due to the condensed structure of heterochromatin, and unresolved replication barriers and/or asynchronous replication may result in DNA damage such as DNA double-strand breaks (Leach et al., 2000). Overstimulation of cell proliferation pathways has been shown to generate replication stress and DNA double-strand breaks at regions difficult to replicate, due to the conflict between unscheduled DNA synthesis and uncoordinated pre-replicative complex assembly (Bartkova et al., 2005; Gorgoulis et al., 2005). Indeed,

p16^{INK4a} deletion, which promotes cell proliferation, is detected in both of our telomerase-immortalized cell lines (Li et al., 2006; Cheung et al., 2010).

Based on the above information, we suggest the following model to explain centromeric instability. In cells overstimulated to proliferate, centromeric regions are predisposed to spontaneous DNA damage; defective G2 phase may impair the correct repair of the damage, which then manifest as chromosomal breaks or rearrangements. The spontaneous DNA damage and response at or near centromeric regions in G2 checkpoint-defective cells is currently under active investigation in our laboratory.

Extensive centromeric instability is believed to have oncogenic potential in least two ways. First, most centromeric aberrations result in whole-arm losses or gains, which lead to large-scale alterations of gene dosage. Ample amount of data from comparative genomic hybridization showed that whole-arm imbalances are common in tumors (Struski et al., 2002). Second, centromeric heterochromatin encompasses multiple forms of inactive chromatin structure that can lead to gene silencing, so that translocations at centromeric or pericentromeric regions may result in gene deregulation (Dillon and Festenstein, 2002; Perrod and Gasser, 2003). We thus propose that centromeric instability represents one of the basic forms of genomic instability and may play a functional role in cancer development.

The role of G2 checkpoint defect in the manifestation of centromeric instability has important implications for genomic instability in cancer. In the context that low levels of DNA damage can escape normal G2 checkpoint (Deckbar et al., 2007; Lobrich and Jeggo, 2007), it has been shown that G2 checkpoint defect further reduces the efficacy of DNA damage repair (Terzoudi et al., 2005). Our data demonstrate that the G2 checkpoint in

cancer cells is not as stringent as in normal cells. One of the direct causes of G2 checkpoint defect is the overexpression of cyclin B1. In fact, cyclin B1 overexpression has been frequently detected in numerous types of cancer (Ito et al., 2000; Takeno et al., 2002; Yoshida et al., 2004; Nakamura et al., 2005; Suzuki et al., 2007). Multiple pathways are able to up-regulate cyclin B1. One of the well-studied classical pathways is through mutation or inactivation of ATM (Abraham, 2001). Another classical pathway is through inactivation of p53, which can regulate G2 checkpoint through inhibition of cyclin B1 (Innocente et al., 1999), and p53 pathway inactivation has been detected in most cancer (Hanahan and Weinberg, 2000). Furthermore, oncogenes such as H-Ras (Santana et al., 2002), c-Myc (Yin et al., 2001) and the viral oncogene human papillomavirus type 16 E6 (Kaufmann et al., 1997) can also activate cyclin B1. Therefore, the existence of a plethora of pathways leading to the upregulation of cyclin B1, thus G2 checkpoint defect, offers a novel and broad explanation for the common occurrence of centromeric aberrations in cancer cells. Further studies on the up-stream mechanisms underlying the preferential centromeric DNA damage and the role of centromeric instability in early process of cancer development are warranted.

Materials and Methods

Cell culture, chemicals and irradiation

Immortalized and primary normal epithelial cells were cultured as reported (Li et al., 2006; Deng et al., 2008; Cheung et al., 2010). Fibroblasts from A-T patients (obtained from Coriell Cell Repositories) and cancer cells were cultured in DMEM supplemented

with 10% FBS. Informed consents for normal tissue donation were obtained from the patients before surgery. KU55933 (Calbiochem) was dissolved in dimethyl sulfoxide (DMSO). ^{137}Cs γ-ray irradiation was carried out in a GammaCell 220 irradiator (Atomic Energy of Canada Ltd.) at a dose rate of 1 Gy/min.

Retroviral infection

NE2-hTERT and NP460-hTERT cells were infected with retroviral vector pApuro-CyclinB1 or control vector pBabe-puro using 4 μg/ml polybrene (Sigma-Aldrich). The cyclin B1 expression vector was a kind gift from Dr. Prochownik, Pittsburgh, PA (Yin et al., 2001). The pApuro vector was modified from pBabe-puro vector (Takata et al., 1994). Two days after retroviral infection, the cells were selected with 0.5 μg/ml puromycin for 6 days. The resistant cells were pooled for experiments.

RNA interference

ShRNA plasmid against cyclin B1 (pKD-Cyclin B1-v4) and negative control plasmid (pKD-NegCon-v1) were purchased from Millipore. Plasmid transfections were carried out according to the recommended protocols of the company.

Chromosome spreads preparation, SKY, and centromere FISH

The cells in the absence of γ-ray irradiation were analyzed for chromosome aberrations. To accumulate metaphases, cells were treated with colcemid (Sigma-Aldrich, 0.03 μg/ml) for 2 h unless otherwise specified. Chromosome spreads were prepared as described (Deng et al., 2003). SKY and centromere FISH were done sequentially as reported (Deng et al., 2007). The rhodamine-labeled pan-centromere DNA probes (Cambio Ltd.) were used for centromere FISH. One to two hundred metaphases from multiple experiments

were analyzed for detailed chromosome aberrations using SKY and centromere FISH. Only non-clonal aberrations were used to quantify chromosome instability.

G2 checkpoint function analysis

The function of G2 checkpoint was monitored by the decrease in the percentage of mitotic spreads 2 h after 1 Gy γ-ray irradiation relative to un-irradiated control cells (relative mitotic index) (Terzoudi et al., 2005; Deckbar et al., 2007). For each experiment point, at least 5000 cells were counted. Mitotic cells were identified after chromosome spreading (without colcemid treatment).

Western blotting

Ten-microgram protein was separated by SDS-PAGE and blots were prepared on a polyvinylidene fluoride membrane (Amersham). Primary antibodies against cyclin B1 and actin were from Santa Cruz Biotechnology. Antibodies against phosph-cdc2(Thr161) and total cdc2 were from Cell Signaling Technology. The membrane was probed with secondary antibody against peroxidase-conjugated mouse, rabbit, or goat IgG, and the blots were visualized by the enhanced chemiluminescence Western blotting system (Amersham).

Statistical analysis

The two-tailed T-test was used to examine the statistical differences. P values < 0.05 were deemed significant. In all bar graphs, error bars represent standard deviations.

Conflict of Interest

The authors declare no conflict of interest.

Acknowledgements

We thank Dr. Prochownik, Children's Hospital of Pittsburgh, Pittsburgh, PA, for the kind gift of pApuro-CyclinB1 plasmids, and Department of Pediatrics and Adolescent Medicine, The University of Hong Kong, for use of SKY facilities. We also thank Dr. J.C. Tang (Department of Applied Biology and Chemical Technology, The Hong Kong Polytechnic University) and Prof. G. Srivastava (Department of Pathology, The University of Hong Kong) for the SLMT-1 cell line, and Dr. R. Glaser (Department of Medical Microbiology and Immunology, Ohio State University Medical Center) for the HNE-1 cell line; T. Chan, P. Y. Cheung, C. S. Leung, P. Mak, J. Cheung, A. Li and B. Lai for technical assistance. This study was supported by a grant from the Research Grants Council of Hong Kong Special Administrative Region, China, Project No. HKU 7556/06M.

References

Abraham RT. (2001). Cell cycle checkpoint signaling through the ATM and ATR kinases. *Genes Dev* **15**: 2177-2196.

Bartkova J, Horejsi Z, Koed K, Kramer A, Tort F, Zieger K et al. (2005). DNA damage response as a candidate anti-cancer barrier in early human tumorigenesis. *Nature* **434**: 864-870.

Beheshti B, Karaskova J, Park PC, Squire JA, Beatty BG. (2000). Identification of a high frequency of chromosomal rearrangements in the centromeric regions of prostate cancer cell lines by sequential giemsa banding and spectral karyotyping. *Mol Diagn* **5**: 23-32.

Cheung PY, Deng W, Man C, Tse WW, Srivastava G, Law S et al. (2010). Genetic alterations in a telomerase-immortalized human esophageal epithelial cell line: implications for carcinogenesis. *Cancer Lett* **293**: 41-51.

Deckbar D, Birraux J, Krempler A, Tchouandong L, Beucher A, Walker S et al. (2007). Chromosome breakage after G2 checkpoint release. *J Cell Biol* **176**: 749-755.

Deng W, Tsao SW, Guan XY, Cheung AL. (2007). Microtubule breakage is not a major mechanism for resolving end-to-end chromosome fusions generated by telomere dysfunction during the early process of immortalization. *Chromosoma* **116**: 557-568.

Deng W, Tsao SW, Kwok YK, Wong E, Huang XR, Liu S et al. (2008). Transforming growth factor beta1 promotes chromosomal instability in human papillomavirus 16 E6E7-infected cervical epithelial cells. *Cancer Res* **68**: 7200-7209.

Deng W, Tsao SW, Lucas JN, Leung CS, Cheung AL. (2003). A new method for improving metaphase chromosome spreading. *Cytometry A* **51**: 46-51.

Dillon N , Festenstein R. (2002). Unravelling heterochromatin: competition between positive and negative factors regulates accessibility. *Trends Genet* **18**: 252-258.

Ehrlich M. (2002). DNA hypomethylation, cancer, the immunodeficiency, centromeric region instability, facial anomalies syndrome and chromosomal rearrangements. *J Nutr* **132**: 2424S-2429S.

Eichler EE , Sankoff D. (2003). Structural dynamics of eukaryotic chromosome evolution. *Science* **301**: 793-797.

Glaser R, Zhang HY, Yao KT, Zhu HC, Wang FX, Li GY et al. (1989). Two epithelial tumor cell lines (HNE-1 and HONE-1) latently infected with Epstein-Barr virus that were derived from nasopharyngeal carcinomas. *Proc Natl Acad Sci U S A* **86**: 9524-9528.

Gorgoulis VG, Vassiliou LV, Karakaidos P, Zacharatos P, Kotsinas A, Liloglou T et al. (2005). Activation of the DNA damage checkpoint and genomic instability in human precancerous lesions. *Nature* **434**: 907-913.

Hanahan D , Weinberg RA. (2000). The hallmarks of cancer. *Cell* **100**: 57-70.

Innocente SA, Abrahamson JL, Cogswell JP, Lee JM. (1999). p53 regulates a G2 checkpoint through cyclin B1. *Proc Natl Acad Sci U S A* **96**: 2147-2152.

Ito Y, Takeda T, Sakon M, Monden M, Tsujimoto M, Matsuura N. (2000). Expression and prognostic role of cyclin-dependent kinase 1 (cdc2) in hepatocellular carcinoma. *Oncology* **59**: 68-74.

Jin Y, Mertens F, Jin C, Akervall J, Wennerberg J, Gorunova L et al. (1995). Nonrandom chromosome abnormalities in short-term cultured primary squamous cell carcinomas of the head and neck. *Cancer Res* **55**: 3204-3210.

Johansson M, Jin Y, Mandahl N, Hambraeus G, Johansson L, Mitelman F et al. (1995). Cytogenetic analysis of short-term cultured squamous cell carcinomas of the lung. *Cancer Genet Cytogenet* **81**: 46-55.

Kaufmann WK, Schwartz JL, Hurt JC, Byrd LL, Galloway DA, Levedakou E et al. (1997). Inactivation of G2 checkpoint function and chromosomal destabilization are linked in human fibroblasts expressing human papillomavirus type 16 E6. *Cell Growth Differ* **8**: 1105-1114.

Kojis TL, Schreck RR, Gatti RA, Sparkes RS. (1989). Tissue specificity of chromosomal rearrangements in ataxia-telangiectasia. *Hum Genet* **83**: 347-352.

1 Leach TJ, Chotkowski HL, Wotring MG, Dilwith RL, Glaser RL. (2000). Replication of
2 heterochromatin and structure of polytene chromosomes. *Mol Cell Biol* **20**: 6308-6316.

3 Li HM, Man C, Jin Y, Deng W, Yip YL, Feng HC et al. (2006). Molecular and
4 cytogenetic changes involved in the immortalization of nasopharyngeal epithelial cells by
5 telomerase. *Int J Cancer* **119**: 1567-1576.

6 Lobrich M , Jeggo PA. (2007). The impact of a negligent G2/M checkpoint on genomic
7 instability and cancer induction. *Nat Rev Cancer* **7**: 861-869.

8 Nakamura N, Yamamoto H, Yao T, Oda Y, Nishiyama K, Imamura M et al. (2005).
9 Prognostic significance of expressions of cell-cycle regulatory proteins in gastrointestinal
10 stromal tumor and the relevance of the risk grade. *Hum Pathol* **36**: 828-837.

11 Padilla-Nash HM, Heselmeyer-Haddad K, Wangsa D, Zhang H, Ghadimi BM, Macville
12 M et al. (2001). Jumping translocations are common in solid tumor cell lines and result in
13 recurrent fusions of whole chromosome arms. *Genes Chromosomes Cancer* **30**: 349-363.

14 Pandita TK. (2002). ATM function and telomere stability. *Oncogene* **21**: 611-618.

15 Perrod S , Gasser SM. (2003). Long-range silencing and position effects at telomeres and
16 centromeres: parallels and differences. *Cell Mol Life Sci* **60**: 2303-2318.

Pincheira J , Lopez-Saez JF. (1991). Effects of caffeine and cycloheximide during G2 prophase in control and X-ray-irradiated human lymphocytes. *Mutat Res* **251**: 71-77.

Rainey MD, Charlton ME, Stanton RV, Kastan MB. (2008). Transient inhibition of ATM kinase is sufficient to enhance cellular sensitivity to ionizing radiation. *Cancer Res* **68**: 7466-7474.

Santana C, Ortega E, Garcia-Carranca A. (2002). Oncogenic H-ras induces cyclin B1 expression in a p53-independent manner. *Mutat Res* **508**: 49-58.

Stewenius Y, Gorunova L, Jonson T, Larsson N, Hoglund M, Mandahl N et al. (2005). Structural and numerical chromosome changes in colon cancer develop through telomere-mediated anaphase bridges, not through mitotic multipolarity. *Proc Natl Acad Sci U S A* **102**: 5541-5546.

Struski S, Doco-Fenzy M, Cornillet-Lefebvre P. (2002). Compilation of published comparative genomic hybridization studies. *Cancer Genet Cytogenet* **135**: 63-90.

Suzuki T, Urano T, Miki Y, Moriya T, Akahira J, Ishida T et al. (2007). Nuclear cyclin B1 in human breast carcinoma as a potent prognostic factor. *Cancer Sci* **98**: 644-651.

Takata M, Sabe H, Hata A, Inazu T, Homma Y, Nukada T et al. (1994). Tyrosine kinases Lyn and Syk regulate B cell receptor-coupled Ca2+ mobilization through distinct pathways. *EMBO J* **13**: 1341-1349.

Takeno S, Noguchi T, Kikuchi R, Uchida Y, Yokoyama S, Muller W. (2002). Prognostic value of cyclin B1 in patients with esophageal squamous cell carcinoma. *Cancer* **94**: 2874-2881.

Tang JC, Wan TS, Wong N, Pang E, Lam KY, Law SY et al. (2001). Establishment and characterization of a new xenograft-derived human esophageal squamous cell carcinoma cell line SLMT-1 of Chinese origin. *Cancer Genet Cytogenet* **124**: 36-41.

Terzoudi GI, Manola KN, Pantelias GE, Iliakis G. (2005). Checkpoint abrogation in G2 compromises repair of chromosomal breaks in ataxia telangiectasia cells. *Cancer Res* **65**: 11292-11296.

White JS, Choi S, Bakkenist CJ. (2008). Irreversible chromosome damage accumulates rapidly in the absence of ATM kinase activity. *Cell Cycle* **7**: 1277-1284.

Wong N, Lai P, Pang E, Leung TW, Lau JW, Johnson PJ. (2000). A comprehensive karyotypic study on human hepatocellular carcinoma by spectral karyotyping. *Hepatology* **32**: 1060-1068.

Xu B, Kim ST, Lim DS, Kastan MB. (2002). Two molecularly distinct G(2)/M checkpoints are induced by ionizing irradiation. *Mol Cell Biol* **22**: 1049-1059.

Yin XY, Grove L, Datta NS, Katula K, Long MW, Prochownik EV. (2001). Inverse regulation of cyclin B1 by c-Myc and p53 and induction of tetraploidy by cyclin B1 overexpression. *Cancer Res* **61**: 6487-6493.

Yoshida T, Tanaka S, Mogi A, Shitara Y, Kuwano H. (2004). The clinical significance of Cyclin B1 and Wee1 expression in non-small-cell lung cancer. *Ann Oncol* **15**: 252-256.

Zhu D, Ma MS, Zhao RZ, Li MY. (1995). Centromere spreading and centromeric aberrations in ovarian tumors. *Cancer Genet Cytogenet* **80**: 63-65.

Table 1. Statistical analysis of ratios of centromeric to non-centromeric aberrations in KU55933-treated and A-T cells

	Metaphases analyzed	R* (ratio of centromeric aberrations to non-centromeric aberrations) ± standard deviation	*P* value (compared with R based on random assumption)
NE2-hTERT (KU55933 2.5 h)	200	1.83 ± 0.62	< 0.02
NE2-hTERT (KU55955, 48 h)	200	1.93 ± 0.64	< 0.01
NP460-hTERT (KU55933, 2.5 h)	200	1.60 ± 0.52	< 0.05
NP460-hTERT (KU55933, 48 h)	200	2.00 ± 0.64	< 0.01
AG02496	100	1.39 ± 0.38	< 0.005
AG04405	100	1.48 ± 0.36	< 0.001

* Calculated according to the following formula: $R = A \div B$

$$(\sigma R/R)^2 = (\sigma A/A)^2 + (\sigma B/B)^2$$

where σR/R, σA/A and σB/B are relative standard deviation of R, A and B, respectively. A (frequency of centromeric aberrations), σA (standard deviation of A), B (frequency of non-centromeric aberrations), and σB (standard deviation of B) were from data in Figures 4b and 4d. The value of R under random assumption is 0.27.

Figure legends

Figure 1. **Cyclin B1 overexpression and G2 checkpoint function.** (a) Western blot analysis and (b) Relative mitotic indices expressed as percentages of mitotic cells 2 h after irradiation relative to un-irradiated cells.

Figure 2. Frequencies of non-clonal chromosome aberrations per 100 metaphases analyzed using SKY and centromere FISH. $*P < 0.05$.

Figure 3. Cytogenetic analysis of chromosomal aberrations. Left, middle and right images show SKY, inverse DAPI, and centromere FISH signals of the same metaphase, respectively. Arrows indicate aberrant chromosome arms. (a) Examples of centromeric aberrations in telomerase-immortalized cells overexpressing cyclin B1. Arrow-heads indicate centromeres at the broken ends or chromosome rejoining points. (b) Example of fusion between a centromeric end and a telomeric end in AG02496 cells. Arrow-head indicates the fusion point between a centromere and a telomeric end of another chromosome.

Figure 4. Effect of KU55933 (KU) treatment and ATM mutation on G2 checkpoint and chromosome instability. (a) Relative mitotic indices (percentages of mitotic cells 2 h after irrdiation relative to un-irradiated cells). (b) Frequencies of non-clonal chromosome aberrations per 100 metaphases after DMSO or KU55933 treatment. Two hundred metaphases were analyzed for DMSO- or KU55933-treated cells. (c) Comparison between fibroblasts from A-T patients and normal donors for relative mitotic indices after irradiation. (d) The frequencies of spontaneous non-clonal chromosome

aberrations in 100 fibroblasts from A-T patients and normal donors. *$P < 0.05$, **$P < 0.01$, ***$P < 0.001$ for ratio of centromeric aberrations to non-centromeric aberrations compared with 0.27 which is the expected value based on random assumption.

Figure 1 (Deng W et al)

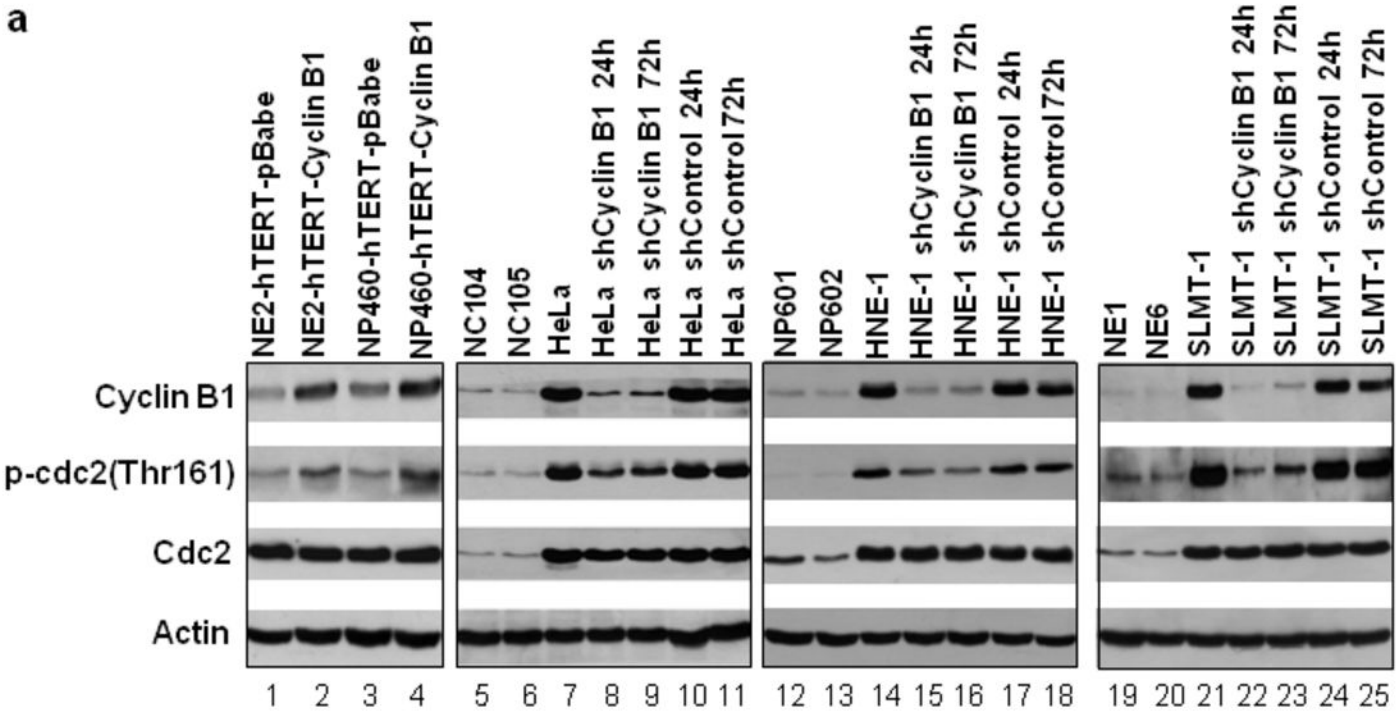

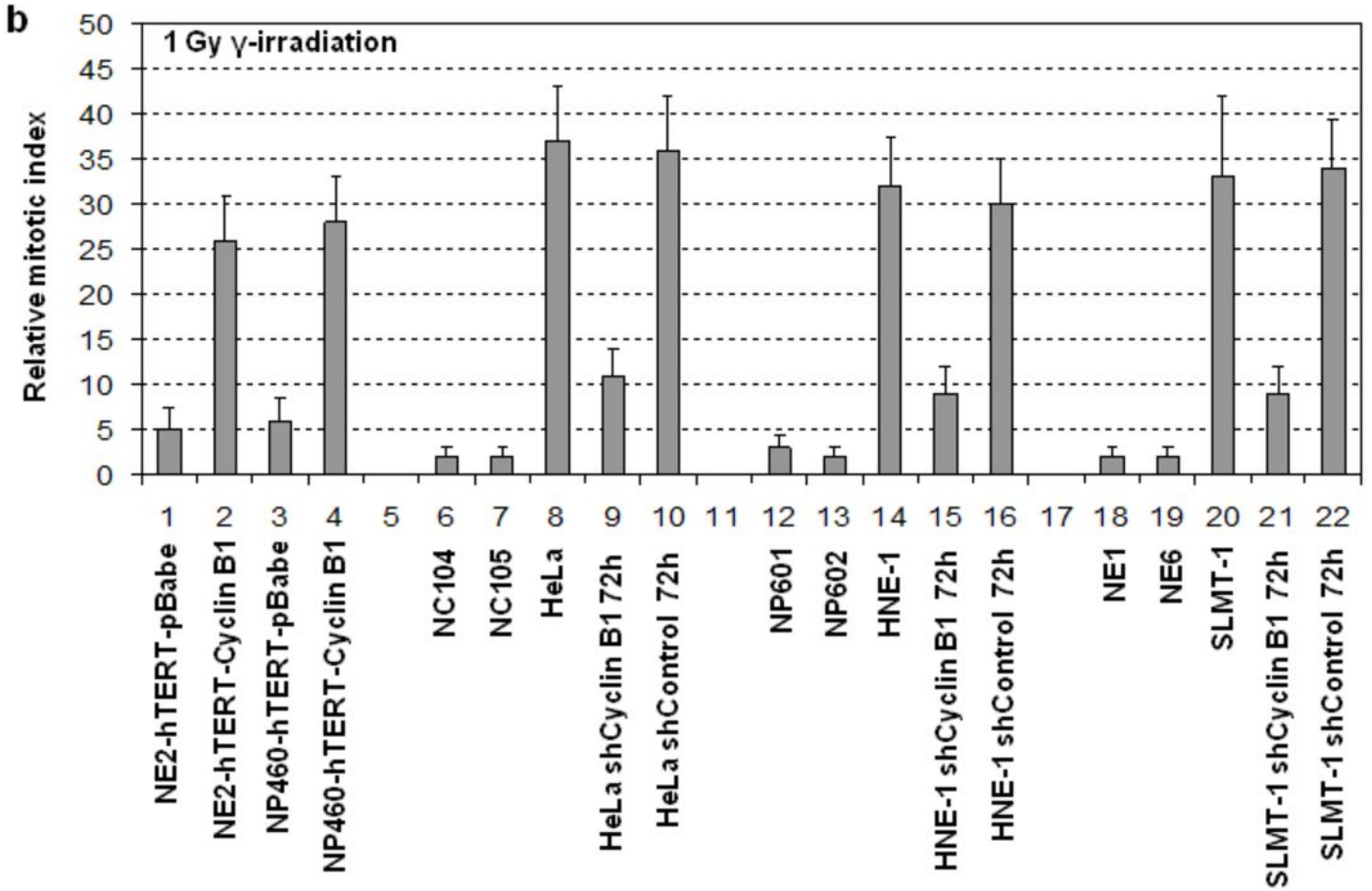

Figure 2 (Deng W et al)

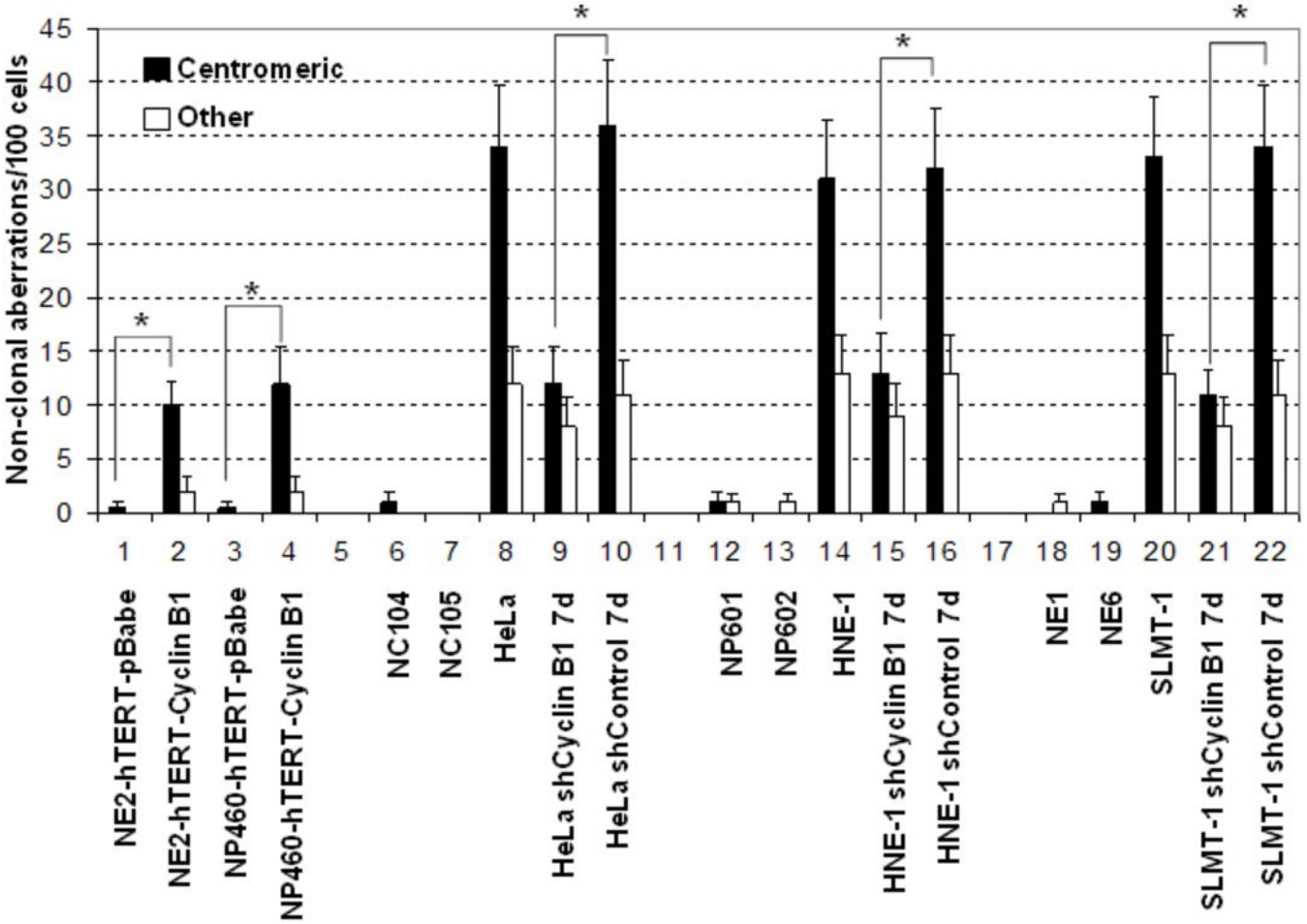

Figure 3 (Deng W et al)

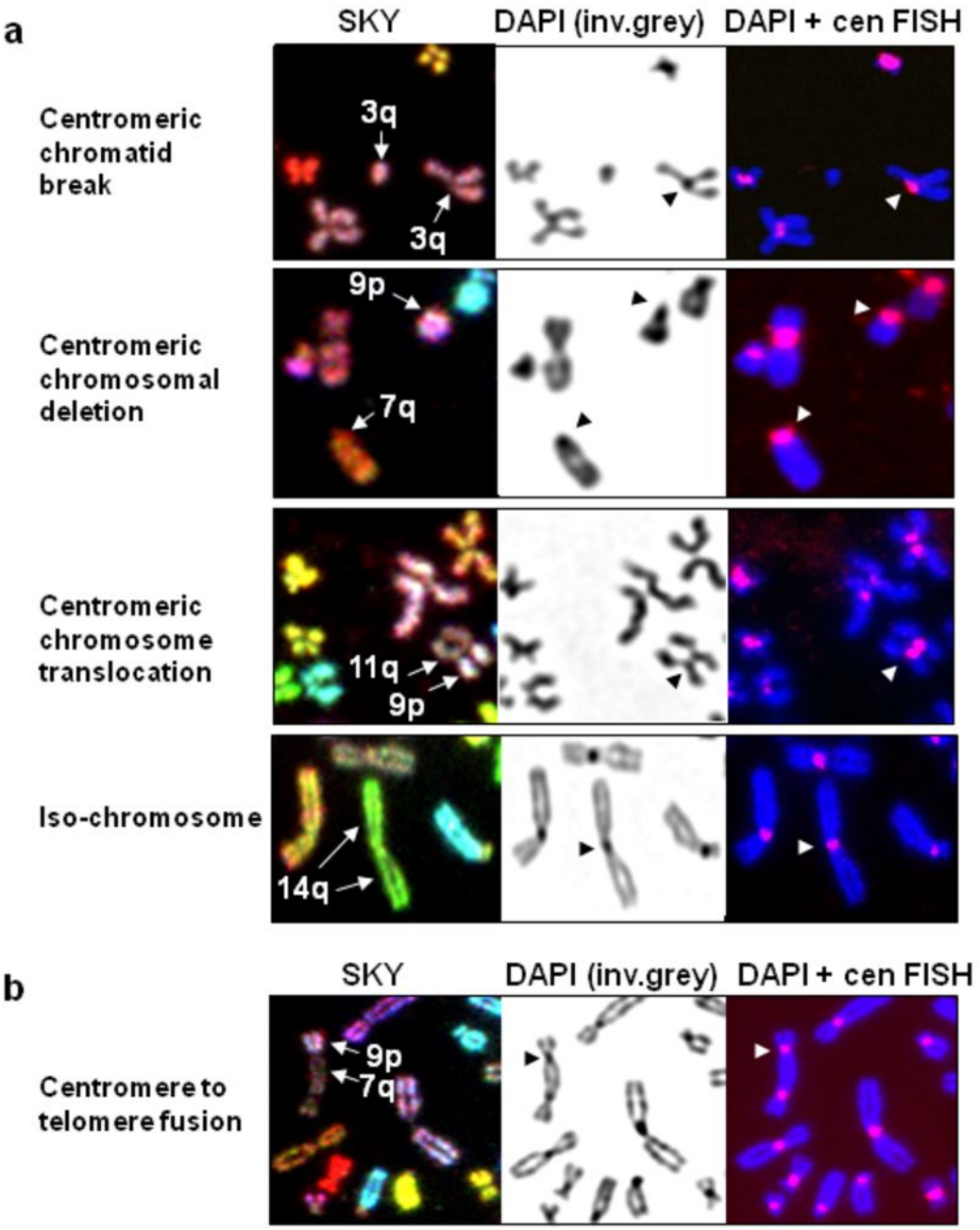

Figure 4 (Deng W et al)